

## Extension of Heat Pump/Heat Engine Principles to Distillation Column Analysis

Olakunle, M.S.<sup>a, 1</sup>, Adefila, S.S.<sup>b, 2</sup>, Olawale, A.S.<sup>c, 3</sup> and Bugaje, I.M.<sup>d, 4</sup>

<sup>A,b,c</sup> Department of Chemical Engineering, Ahmadu Bello University, Zaria, Nigeria

<sup>D</sup> National Research Institute for Chemical Technology (NARICT), Zaria, Nigeria.

---

**ABSTRACT:** A 10-staged conventional binary distillation (using ethanol/water system) operation was analyzed with thermodynamic principles in this work. Use was made of the temperature, composition and enthalpy profiles obtained from the converged simulation of distillation operations obtained from the Aspen Plus and Aspen Hysys simulators. Since all processes in nature are essentially composites of steps of transformation of energy from one form to another, an extension of the application of the simple heat pump/heat engine analysis to the analysis of distillation operation was also investigated. Whereas a distillation column is a heat engine on a global and stand-alone basis, the plate-to-plate distillation operation was seen to be akin to the operation of a reverse absorption heat pump. A similar Chebyshev X,Y Rational Order 5/6 model equation was found to represent the two operations very well, with residual errors ranging between  $\pm 1.5\%$  for the absorption heat pump operation model and  $\pm 3.5\%$  for the distillation operation model using the binary ethanol/water system.

**KEYWORDS:** Absorption heat pump, distillation, co-efficient of performance, analysis by analogy

---

### I. INTRODUCTION

Distillation process has over the years been depicted of being energy intensive (US DOE, 1984, Ognisty, 1995), with the 'energy consuming component' locked in a 'black box'! In the meantime, an endless quest towards improving the economics of the process continued due to the enormous amount of energy utilization and significant capital outlay it requires. Various options are currently being explored in the quest towards energy conservation and recovery (Demirel 2004, 2006; Pinto et al. 2011). Optimization techniques, like pinch and exergy analyses have been developed by several researchers (Dhole and Linnhoff, 1993; Rashad and El Maihy, 2009; Yuelong et al. 2010; Vuckovic et al., 2012) to tackle this high energy utilization problem, but still the thermal efficiencies of stand-alone distillation columns (DCs) are found to be low (Cengel and Boles, 2007). However, the overall operation of a DC succinctly represents that of a heat engine (Ognisty, 1995)– work (High Grade Energy – HGE) generating - and the concurrent plate to plate operation of the DC could be likened to the operation of an absorption heat pump – HGE consuming. Meanwhile, heat pumps and heat engines are easily amenable to thermodynamic analyses (Adefila, 1983). Thus the 'black box' of the distillation process, which apparently lies in its HGE generation cum consumption should be subjectable to identical easy analyses as these two common systems, towards the resolution of their inherent resistivities. The results of these analyses should be applicable to both, enabling distillation systems easier to design and making the operation better manageable for improved thermal efficiency. Earlier conceptual analyses on thermal systems (Dhole and Linnhoff, 1993) produced paradigm shifting impact. Therefore, in this work, attempts were made to establish analogies between critical units in distillation column and the heat engine/heat pump systems. This was aimed at obtaining a more informed understanding of energy transformations in distillation process.

### II. BACKGROUND

Heat pump refers to a device which raises the quality (potential) of heat energy from a low temperature level to heat energy at a higher temperature level, using a relatively small quantity of HGE. Olawale and Adefila (2011, 2012) developed simplified generalized performance equations for vapour compression heat pumps analysis. The models proved to be very useful in the simplified analysis of heat pump systems. Earlier, Holland et al (1981) presented extensive literature of various energy cycles within the heat pump system, while Adefila (1983) and Bugaje (1987) discussed a very detailed classification of heat pumps and their corresponding analysis. In absorption heat pumps (AHP), Figure 1, an expansion valve is used for the expansion from condensing to evaporating pressure. However, the compression process, and thus the addition of primary energy, is achieved by a thermodynamic system without a mechanical compressor. The drive of the AHP consists of a circuit in which the working fluid is absorbed by an absorbent at a lower pressure and is separated again from it by adding heat at a higher pressure and returns into the normal heat pump cycle. The only mechanical driven component in the circuit is the solution pump.

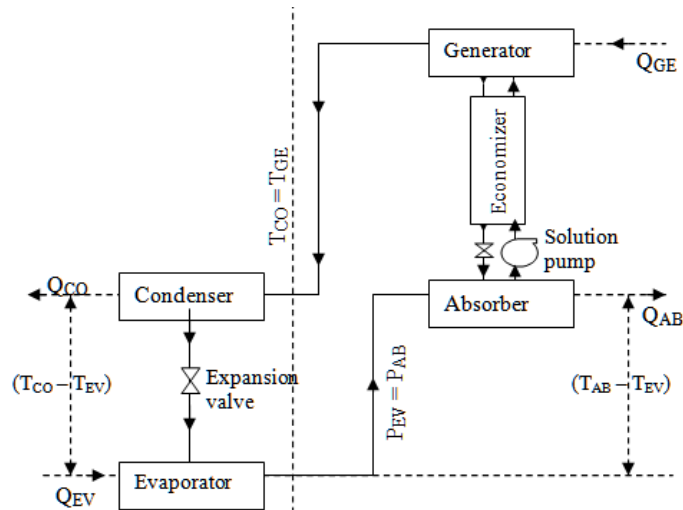


Figure 1. A Conventional Absorption Heat Pump

After evaporation, the working fluid is absorbed by the absorbent in the absorber accompanied by a rejection of heat  $Q_{AB}$  to the surroundings. In this mixture, the evaporator pressure becomes the partial pressure of the working fluid. The enriched solution is compressed to the pressure in the generator by a pump and heated to a temperature  $T_{GE}$ . At the higher temperature, the solubility of the working fluid in the absorbent is appreciably smaller, and the heat received  $Q_{GE}$  results in the removal of the vapour (working fluid) from solution. The working fluid, now separated from the solution, passes to the condenser. The depleted solution is expanded to the pressure of the absorber by an expansion valve and can now again absorb working fluid.

The Coefficient of Performance (COP) for the conventional absorption heat pump, depending on the targeted effect, can be written as:

$$(COP)_{AHA} = \frac{Q_{CO} + Q_{AB}}{(Q_{GE})} \quad \text{for heating} \quad 1$$

and

$$(COP)_{ACLA} = \frac{Q_{EV}}{(Q_{GE})} \quad \text{for cooling} \quad 2$$

Comparison of the actual COP can be made with the theoretical Carnot efficiency. Figure 2 is a schematic of a Carnot absorption heat pump viewed as composing of a Carnot heat engine, on the right hand side, and a reversed Carnot heat engine (Carnot heat pump) on the left hand side.

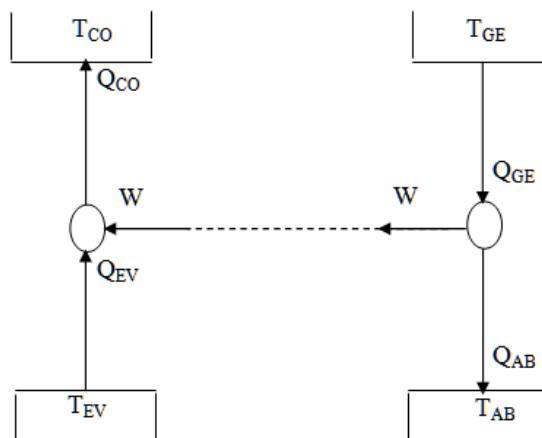


Figure 2: Carnot Absorption Cycle Principle

According to the cycle, the minimum amount of work  $W$ , required to operate a heat pump for cooling, at an absolute temperature of  $T_{EV}$ , when ambient temperature is  $T_{CO}$  is

$$W = \left[ \frac{T_{CO} - T_{EV}}{T_{EV}} \right] Q_{EV} \quad 3$$

Likewise, the minimum quantity of heat energy required to contain an amount of work  $W$ , in a Carnot heat engine is,

$$Q_{GE} = \left[ \frac{T_{GE}}{T_{GE} - T_{AB}} \right] W \quad 4$$

Consequently, the quantity of heat at the high temperature  $T_{GE}$  required to effect a cooling capacity of  $Q_{EV}$  is obtained by combining Equations 3 and 4 to give,

$$Q_{GE} = \left[ \frac{T_{GE}}{T_{GE} - T_{AB}} \right] \left[ \frac{T_{CO} - T_{EV}}{T_{EV}} \right] Q_{EV} \quad 5$$

Thus, with reference to Equation 5, the COP for the heating mode is given as,

$$(COP)_{AH} = \frac{T_{EV}}{T_{GE}} \left[ \frac{T_{GE} - T_{AB}}{T_{CO} - T_{EV}} \right] + 1 \quad 6$$

Adefila (1983) derived a pseudo-ideal model for calculating the maximum obtainable COP for the heating mode of a high temperature CAHP system. The  $(COP)_{AHMO}$  is equivalent to Rankine (COP) in vapour compression heat pump systems, and the mathematical relation between  $(COP)_{AHMO}$  and the absorbent and working fluid in the system found through mass and energy balances as shown in Figure 3 is given as

$$(COP)_{AHMO} = \frac{H_4 - H_7 + (FR)(H_7 - H_8) + H_1 - H_3}{(FR)(H_5 - H_{10}) + H_1 - H_5} \quad 7$$

where,

$$(FR) = \frac{1 - (X_W)_5}{(X_W)_{10} - (X_W)_5} = \frac{X_{GE}}{X_{GE} - X_{AB}} \quad 8$$

where  $X_{AB}$ ,  $X_{GE}$  are weight percent of solute in solution in the absorber and generator respectively and  $X_W$  is fractional weight of working fluid in solution.

The application of the phase rule shows that

$$(COP)_{AHMO} = (COP)_{AHMO} ((FR), T_{CO}) \quad 9$$

However, the 'thermodynamic compressor' is composite. This is partially elucidated by Equation 8 which shows (FR) to be a function of the absolute concentration of the working fluid mixture in the generator and absorber, and the concentration width. In fact, a more useful form of this Equation is

$$(FR) = (FR) (T_{GE}, P_{CO}/P_{EV}) \quad 10$$

Or  $(FR) = (FR) (T_{AB}, P_{EV}, P_{CO}/P_{EV}) \quad 11$

These expanded equations present very useful basic parameters for the design, evaluation or control of the absorption heat pump system.

### III. METHODOLOGY

#### 2.1 Analysis by Analogy

A cursory look at the plate-to-plate operation of the distillation process and that of the conventional absorption heat pump was critically considered via analysis by analogy to establish the similarities of operations between the two systems. The simultaneous vapourization and condensation processes of the plate-to-plate distillation operation was theoretically compared with the vapourization/absorption and evaporation/condensation processes of the conventional absorption heat pump using the description of the processes shown in Figures 3 and 4. In the conventional absorption heat pump, the absorber/evaporator units are at the same pressure, likewise the condenser/generator combination, though at relatively higher pressure. Thus the generator and the absorber are at different pressure levels; this pressure difference is equilibrated by the presence of the solution pump and the expansion valve which are fixed between the absorber and the generator.

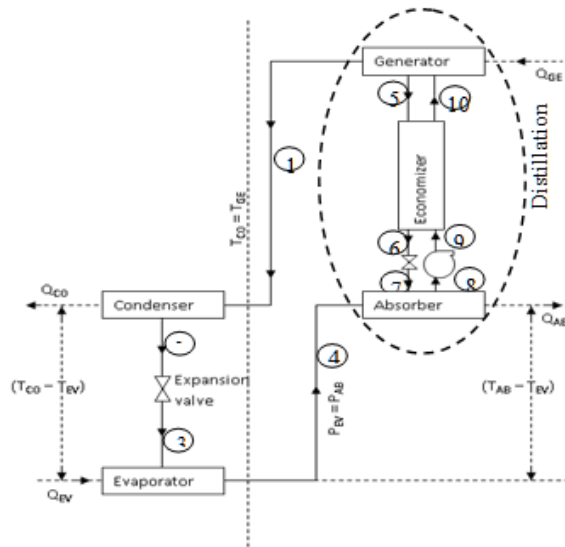


Figure 3: Conventional Absorption Heat Pump

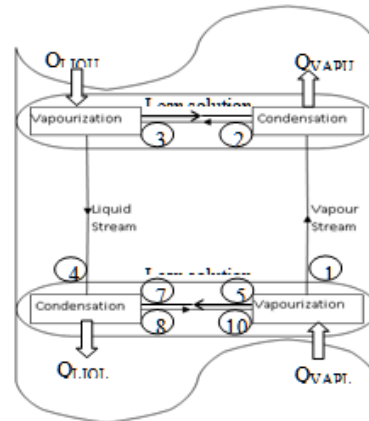


Figure 4: Plate-to-Plate Distillation Operation

## 2.2 Performance evaluation and modelling of a conventional absorption heat pump and distillation operation.

The process flow diagram (PFD) of a conventional absorption heat pump (CAHP) system was set-up as shown in Figure 3 using the Aspen Hysys process simulator. In Figure 5, the absorber of a practical CAHP was conceived to be a combination of a mixer and a cooler. This is so because in the absorber of a practical CAHP, both mixing and condensation processes occur, hence the display of absorber mixer and absorber cooler. Similarly, the generator of a practical CAHP also has both heating and rectification processes occurring within it. This PFD was then used to generate process data for the streams shown in the PFD, which was used to calculate the enthalpies of all the streams in the cycle.

Assumptions made in the simulation were:-

- The Stream no. 2 leaving the rectifier into the condenser was taken to be superheated vapour which possesses high grade energy for delivery in the condenser.
- The Stream no. 5 leaving the evaporator into the absorber was taken to be saturated vapour. This represents the pseudo-ideal condition for the exit stream from the evaporator.
- The simulation runs were limited to a composition range of the working fluid/absorbent (ethanol/water) pair of 0.5 and 0.75 and a temperature range of between 60<sup>0</sup> and 80<sup>0</sup>C. At mixture composition and temperature higher than these, separation would not be effective since ethanol/water mixture forms azeotrope at temperatures above 80<sup>0</sup>C.

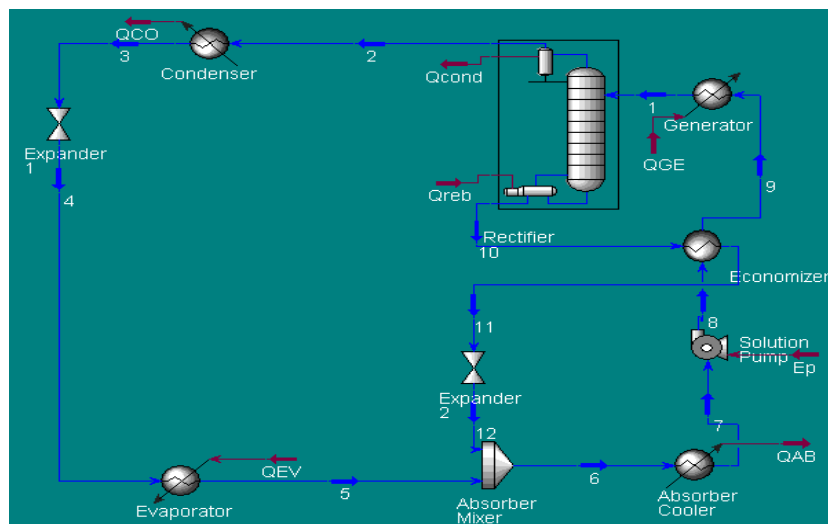


Figure 5: Schematic of a Conventional Absorption Heat Pump

- The Stream no. 3 leaving the condenser into the expander was taken to be saturated liquid.
- The temperature and pressure conditions in the condenser and the evaporator were taken to be constant; hence phase changes from vapour to liquid and from liquid to saturated vapour take place in these units respectively.
- Vapour inlet to the solution pump was avoided.
- The pressure in the generator and the condenser were taken to be the same. Likewise, the pressure in the absorber and the evaporator were the same.

The calculated mass enthalpies were then used to determine the maximum obtainable coefficient of performance ( $COP_{AHMO}$ ) of the system for each runs of the simulated process using the expression of Equations 7 and 8, modified as in Equations 12 and 13 respectively.

$$(COP)_{AHMO} = \frac{H_2 - H_{12} + (FR)(H_{12} - H_7) + H_2 - H_3}{(FR)(H_{10} - H_9) + H_2 - H_{10}} \quad 12$$

where

$$(FR) = \frac{1 - (X_W)_{10}}{(X_W)_9 - (X_W)_{10}} = \frac{X_{GE}}{X_{GE} + X_{AB}} \quad 13$$

where  $X_{AB}$ ,  $X_{GE}$  are weight percent of solute in solution in the absorber and generator respectively and  $X_W$  is fractional weight of working fluid in solution. FR is the fluid ratio.

Aspen-Hysys simulator was also used to simulate a distillation operation for ethanol -water binary system in order to generate data for modelling the distillation operation. The conditions used for the simulation of the distillation operation are as given in Table 2. Several simulation runs were undertaken varying the feed composition from 0.1 to 0.9 ethanol mole fraction. The data generated were used to develop a model which was compared with that for the CAHP for its easy extension for the analysis of distillation operation. The effect of the feed stream temperature on the COP equivalent of the distillation column were also estimated from the data based on the comparison between the distillation operation and the conventional absorption heat pump system.

Table 2: Distillation Operating Conditions

S/No.	Parameters	Simulation Value
1	Number of Stages	10
2	Feed Rate, litre/s	$9.5 \times 10^{-4}$
3	Feed Rate, mol/s	0.04161
4	Feed Pressure, $10^5$ Pa	1.01325
5	Feed Temperature, K	302.45
6	Feed Stage	5
7	Condenser Pressure, $10^5$ Pa	1.0111
8	Pressure Drop, Stage 2-10, Pa	980
9	Distillate Rate, mol/s	0.00205
10	Reflux Ratio	5
11	Feed Mole Fraction	0.1
12	Condenser Type	Total

## IV. RESULTS AND DISCUSSION

### 3.1 Analysis by Analogy

The theory of absorption heat pumps is based on thermodynamics of solution; likewise that of distillation. In binary mixtures, each condition of state is determined by three parameters: pressure (P), temperature (T) and solution concentration ( $X_W$ ) in weight fraction of working fluid. A deeper examination of the various operations within the units that constitute the absorption heat pump (i.e the vapourization/absorption processes of the ‘thermodynamic solution circuit’ of the generator/absorber unit, and the evaporation/condensation processes of the ‘vapour flow’ of the evaporator/condenser unit) is very much akin to the simultaneous vapourization/condensation processes of the plate-to-plate distillation operations. Table 3 illustrates the comparative description of the components and processes between the two systems. The vapourization process (in the generator) and the condensation process (in the absorber) of the thermodynamic solution circuit in the CAHP system (shown in the envelope of Figure 3) actually mimic the simultaneous vapourization and condensation processes of the plate-to-plate operation in a distillation column. Whereas the evaporation and condensation processes of the evaporator and the condenser of the CAHP are subsumed in the upper plate vapourization and condensation processes of the distillation operation. Table 3: Comparative Description of the Components and Processes of the Conventional Absorption Heat Pump and the Plate Distillation Operation

S/N	Unit\System	Absorption Heat Pump	Distillation Operation
1	Generator	Vapourization process takes place in the generator in an absorption heat pump system. The rich solution (10) rising from the absorber through the solution pump and the economizer is heated by the high grade energy $Q_{GE}$ supplied to the generator. The more volatile component (1) of the rich solution is vapourized leaving a lean solution (5) which is returned back to the absorber via an expander for another vapour intake.	The reboiler of the distillation column is akin to the generator. On a plate-to-plate consideration, the lower plate serves as the generator, because it is present at a higher energy value due to the high grade energy, $Q_{VAPL}$ vapour entering the plate from the reboiler. The more volatile component of the liquid mixture (10) flowing down the downcomer of the column is vapourized by the high grade energy vapour. The vapourized component (1) then rises up the column to increase the composition of the more volatile component on the upper plate, and also provide the work energy needed for the component separation on that plate
2	Absorber	Condensation process takes place in the absorber. The lean solution (5) flows from the generator through the economizer (6) and the expander (7) takes up the vapour from the evaporator (4) thereby producing a rich solution (8) that is pumped to the generator via the economizer. The condensation process releases the heat of condensation and mixing $Q_{AB}$ . This heat of mixing is often reflected in the temperature value of the exiting rich solution (8) as determined by the $C_p$ values of the mixing streams	A lean solution (5) on the plate flows to the downcomer (7) where it then flows downward to a lower plate for vapour intake. This lean solution mixes with the vapour rising from a lower plate causing condensation of that vapour stream, thereby releasing the heat of mixing, $Q_{LIQL}$ . The condensing and evaporating processes are both subsumed in the upper plates of the distillation column. The upper plate of an equilibrium staged-column serves as the condenser in that it receives the vapour coming from the reboiler (i.e. lower plate in this case). As the vapour enters the plate, it mixes with the liquid on that plate and condenses by losing heat $Q$ which is used to perform the work of separation on that plate. Since there is simultaneous condensation and vapourization on the plate.
3	Condenser	The vapour from the generator (1) is condensed. The high grade energy $Q_{CO}$ from this condensation process could be used to heat up process stream, which is a type of fluid work done. The low grade vapour (2) emanating from the unit is then expanded and flows to the evaporator	Likewise, the evaporator is also subsumed in the upper plate, probably in the vapourization unit of the upper plate. Here, $Q_{LIQU}$ , a lower grade energy compared to $Q_{COLL}$ , is supplied by the lean solution flowing into that plate from an upper plate. This energy is used to vapourize some of the more volatile component on the plate, which does increase the purity of the vapour component.
4	Evaporator	The low pressure, low grade heat vapour stream (3) flows into the evaporator, where it absorbs low grade energy $Q_{EV}$ that slightly raises its energy to a condition for the absorber intake of the vapour (4).	

It follows therefore, that compared to the CAHP system the distillation operation would be expected to give a higher efficiency in terms of energy utilization. This is due to the absence of the hardware components of the condenser, the solution pump, the economizer and the evaporator, which on their own introduce additional irreversibility to the entire process. The low pressure liquid stream flowing downwards from an upper plate possesses kinetic energy and hydrostatic head with which it upgrades its low pressure to that of the incoming high pressure vapour stream flowing upward from the plate beneath. With the pressure balance on the plate, proper mixing of the vapour and liquid streams is achieved. Concurrently, the effective collapse of the vapour droplets into liquid during condensation and the sudden volume expansion due to vapourization of liquid molecule, like the 'tsunami effect', also contribute to make the mixing very effective. This effective mixing therefore brings the liquid and vapour streams on the plate into intimate contact creating opportunity for mass and energy transfer as a result of the concentration and energy gradients between the mixing streams. During

mixing both heat of mixing and heat of condensation, a type of  $Q_{AB}$  and  $Q_{CO}$  are generated, which are probably used to vapourize the most volatile component (MVC) of the liquid stream. The vapourization of the MVC from the liquid stream brings about separation on that plate. This operation continues up the column, giving rise to a vapour stream that gets richer in the MVC, while the liquid flowing downwards gets leaner in the MVC.

From the foregoing therefore, the processes of vapourization and absorption in the CAHP system are comparable to the plate-to-plate operation of the distillation process; the already developed and established models of the CAHP system can therefore be extended to analyze the performance of distillation operation.

In the CAHP, the major objectives are the cooling and heating effects of the system, hence the calculation of coefficient of performance for both cooling ( $COP_{CL}$ ) and heating ( $COP_H$ ) respectively. However, since the condenser/evaporator processes of the vapour unit of the CAHP system is subsumed in the upper plate of a distillation operation, the high grade energy intake of the generator as in the reboiler, (akin to a lower plate (of high P and T) of a distillation operation) could only have been used to deliver energy that would have been used to effect separation. From the comparison in Table 3 therefore, it can be seen that:

- $Q_{GE} = Q_{VAPL}$        $H_{GE}$  associated with the vapour from the lower plate
- $Q_{AB} = Q_{LIQL}$       Heat energy associated with the liquid from the lower plate
- $Q_{CO} = Q_{VAPU}$       Heat energy associated with the vapour from the upper plate
- $Q_{EV} = Q_{LIQU}$       Heat energy associated with the liquid from the upper plate

The  $(COP)_{AHMO}$  model equation of the CAHP system is therefore the most suitable model applicable to plate-to-plate distillation operation.

### 3.2 Performance evaluation and modelling of a conventional absorption heat pump and distillation operation.

The results of the effect of generator temperature on the  $COP_{AHMO}$  of a CAHP using ethanol-water pair evaluated at different rectifier temperature and molar composition of the ethanol are as shown in Figures 6 and 7.

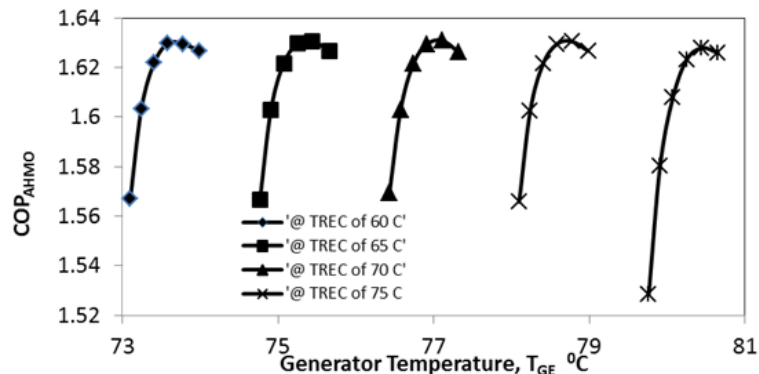


Figure 6:  $COP_{AHMO}$  versus  $T_{GE}$  at different  $T_{REC}$

$T_{GE}$  is the average temperature of all the streams involved in the vapour generating processes of the generator unit. Similarly, the condenser temperature,  $T_{CO}$  is the average temperature of the streams linked to the condenser. The corresponding temperature lift,  $T_{LIFT}$ , for these plots is approximately  $31.3^\circ C$ , while the evaporator temperature,  $T_{EV}$  was  $47^\circ C$ . The concentration gap varies between 0.06 and 0.165. A close examination of Figure 6 shows that the performance of the CAHP increases with increase in  $T_{GE}$ , irrespective of the rectifier entrance temperature. A maximum  $COP_{AHMO}$  value of about 1.6309 is attained at  $T_{REC}$  of  $70^\circ C$ , which suggest the optimum condition to operate the CAHP system. All the plots followed the same trend in which there was an increase in  $COP_{AHMO}$  with slight increase in  $T_{GE}$ , which continued until it reached a maximum and then began to diminish. Thus beyond this maximum points, operating the system at higher  $T_{GE}$  will no longer be economical as higher grade energy supplied to the generator will yield a lesser output of the delivered heat at the condenser. Figure 7 shows the plot of  $COP_{AHMO}$  versus  $T_{GE}$  but at different values of the molar composition of the working fluid/absorbent mixture. It could be seen that operating the system at 0.55 molar composition of the mixture will deliver the best performance. Below and above this will also not be economical in terms of performance for the system. However, a similar trend of the plots was observed in which there was a little increase in the performance of the system as the  $T_{GE}$  increased until it peaked at about  $T_{GE}$  of  $78^\circ C$  before a diminishing return set in. This suggests that the optimal  $T_{GE}$  would be  $78^\circ C$  beyond which the process would be uneconomical.

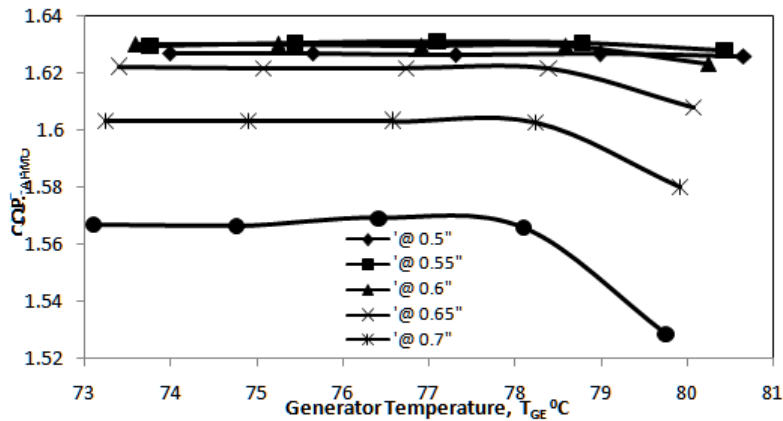


Figure 7: COP<sub>AHMO</sub> versus T<sub>GE</sub> at different ethanol/water Mole Fractions.

However, Thermal Economics suggests that operating at 74<sup>0</sup>C is sufficient point on the COP<sub>AHMO</sub>-T<sub>GE</sub> Plateau. Furthermore, the COP<sub>AHMO</sub> values peaked at a mole fraction of the ethanol/water system of 0.55 and then declined on higher molar fraction. Thus, the 0.55 mole fraction of the ethanol/water mixture and T<sub>GE</sub> of 74<sup>0</sup>C would yield the most economical COP<sub>AHMO</sub>. These, combined with the results in Figure 6 put Full Thermal Economics at 0.55 mole fraction of the ethanol/water mixture, T<sub>GE</sub> of 74<sup>0</sup>C and and T<sub>REC</sub> 60<sup>0</sup>C. This observation for the ethanol/water system of the CAHP operation agrees with literature data in which Adefila (1983) presented the graph of COP<sub>AHMO</sub> versus T<sub>GE</sub> for LiBr/H<sub>2</sub>O CAHP system, in which a similar trend was obtained. Models developed provide an easy extension of the heat pump/heat engine principle to distillation operation, based on earlier comparison between the two systems. The first model developed for CAHP was that which relates the concentration gap DX of the solution unit as a function of stream enthalpies (H<sub>2</sub> and H<sub>5</sub>), Equation 14.

$$Z = \frac{a + dT_1(x') + eT_1(y') + hT_2(x') + iT_2(y') + lT_3(x') + mT_3(y') + pT_4(x') + qT_4(y') + tT_5(x') + uT_5(y')}{1 + bT_1(x') + cT_1(y') + fT_2(x') + gT_2(y') + jT_3(x') + kT_3(y') + nT_4(x') + oT_4(y') + rT_5(x') + sT_5(y') + vT_6(x') + aaT_6(y')} \quad 14$$

where Z = DX, x' = H<sub>5</sub> and y' = H<sub>2</sub>

Figure 8 shows the parity and residual plots and the parameter values for the compositional changes (DX) model for the absorption heat pump working on ethanol-water binary mixture.

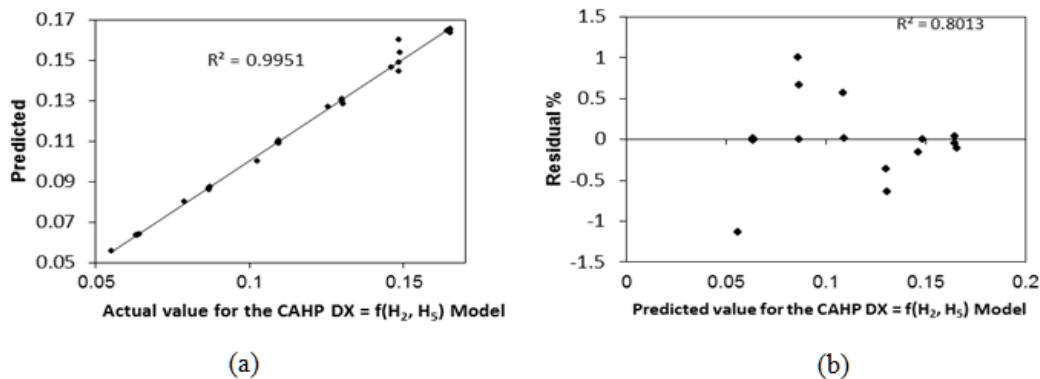


Figure 8(a and b) Parity and Regression Plots for the CAHP [DX = f (H<sub>2</sub>, H<sub>5</sub>) Model

The model developed for the distillation operation is as shown in Equation 15. The model is a Chebyshev X,Y Rational Order 5/6, a type of [DX = f(H<sub>A</sub>,h<sub>A</sub>)] like Equation 14.

$$Z = \frac{a + dT_1(x) + eT_1(y) + hT_2(x) + iT_2(y) + lT_3(x) + mT_3(y) + pT_4(x) + qT_4(y) + tT_5(x) + uT_5(y)}{1 + bT_1(x) + cT_1(y) + fT_2(x) + gT_2(y) + jT_3(x) + kT_3(y) + nT_4(x) + oT_4(y) + rT_5(x) + sT_5(y) + vT_6(x) + aaT_6(y)} \quad 15$$



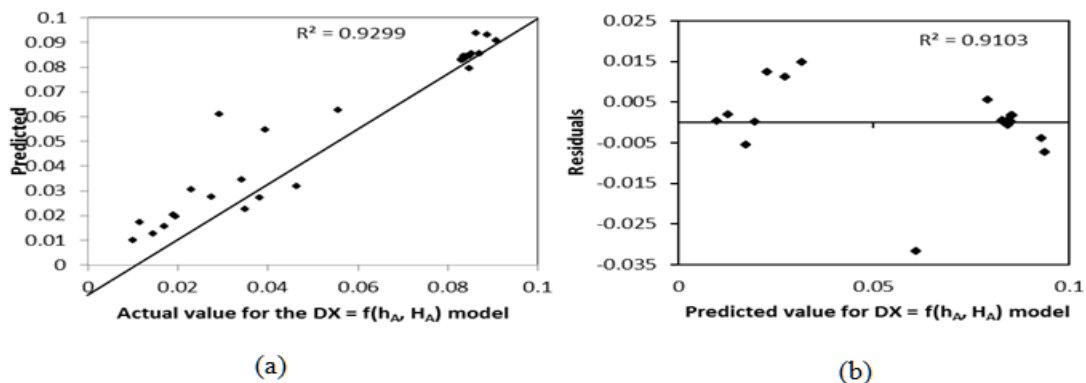


Figure 9(a and b) Parity and Regression Plots for the Distillation [DX = f(h<sub>A</sub>, H<sub>A</sub>) Model

The selection of the variables for the models were based on the earlier comparison between the CAHP and the distillation column, (Figures 3 and 4 and Table 3). Model equation relating concentration gap DX as a function of stream enthalpies (H<sub>2</sub> and H<sub>5</sub>) developed for the CAHP(Equation 14) has a coefficient of determination, r<sup>2</sup> of 0.9948, a fit standard error of 0.00528 and F-Stat value of 61.3194. These are good statistical values that show that the plot is a good fit of the simulated data. F-Stat value indicates the significance of the model occurring not by chance, even though it has a large r<sup>2</sup> value. The DX is a measure of the difference in composition value of the rich-solution flowing from the absorber into the generator and the lean-solution stream leaving the generator after rectification back into the absorber. The parameter values, the parity and residual plots for the model (Tables 4 and Figure 8) showed a very close approximation of the fit with the data. Thus the model Equation 14 is a good representation of the simulated data.

This concentration gap of the CAHP is akin to the concentration difference between the stream flowing downwards into a plate from an upper plate and that coming out of the plate into a further lower plate of the distillation column. The model equation [DX = f(h<sub>A</sub>, H<sub>A</sub>)] – Equation 15, has the following regression parameters: the coefficient of determination (r<sup>2</sup>), of the model is 0.9271 which is a good fit for the data. The fit standard error and the F-Stat value are 0.01686 and 4.0446 respectively, which are good statistical data for the fit as well. The model parameter values and the regression analysis values (Table4 and Figure 9) also showed that the model is a good fit.

Close examination of the models(Equations 14 and 15)also revealed that the two models are of the same Chebyshev model equation type; Chebyshev X,Y Rational Order 5/6 with slightly different parameters. For the fact that the same Chebyshev models could fit the two thermal systems confirms the similarities between the plate-to-plate operation of the distillation and the operation of the CAHP. Based on the similarities of these models, the distillation column which could be viewed as a cascade of several CAHP can thus be analyzed using the COP<sub>AHMO</sub> as the measure of its stage-to-stage performance. It could then be said that stages where the COP<sub>AHMO</sub> falls below 1 shall indicate regions of lower energy efficiency and vice-versa. It should be noted also that since COP is a measure of the ratio of heat delivered to work energy consumed, the higher the COP value, the more efficient the work energy was utilized in the process, thus resulting in minimal exergy losses within the stage.

Figure10 (a and b) are plots of the distillation COP<sub>AHMO</sub> at varying feed plate locations and feed inlet temperatures. For the inlet feed temperature ranging from 302.45K to 352.45K, and the feed plate location ranging from plate 3 to plate 7, it could be seen that the COP<sub>AHMO</sub> increases with increase in the inlet feed temperature as the feed plate location shifts towards plate 3. At each temperature of the feed, plate 3 gives the highest COP<sub>AHMO</sub> values. COP<sub>AHMO</sub> is a measure of the ratio of the separating effect (i.e. the energy utilized in effecting separation within the column) to the work energy input into the system to drive/achieve the separation. The higher the COP<sub>AHMO</sub> value, the better the energy conversion and the lower the energy wastage.

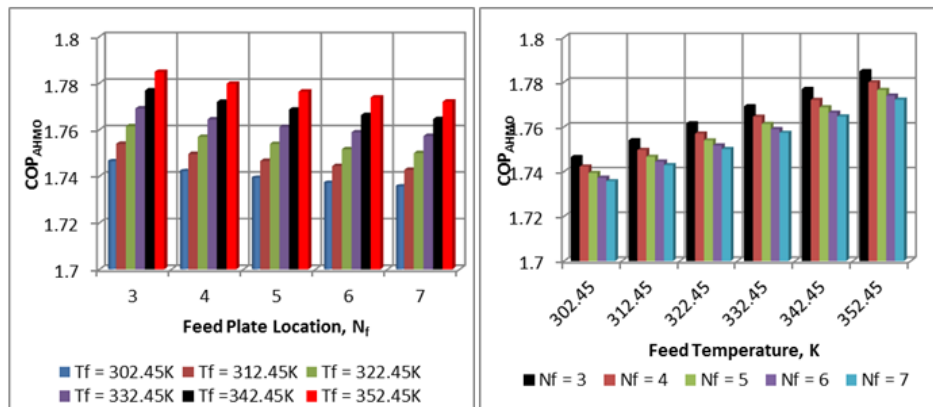


Figure 10(a):  $COP_{AHMO}$  of Distillation at Varying Feed Plate Locations.

Figure 10(b):  $COP_{AHMO}$  of Distillation at Varying Feed Temperatures.

## 5.0 Conclusion

The  $COP_{AHMO}$  model developed could be used to analyze distillation operations, since it has been shown that the operation of an absorption heat pump is similar to that of the plate-to-plate distillation operation. Extending the principles of heat engine and heat pump to distillation operation did provide a better understanding of the energy transformation processes within a distillation column, and will thus make its analysis simpler.

## REFERENCES

- [1]. Adefila, S.S. (1983). *Studies on high temperature heat pump*. (Unpublished Ph.D. Thesis). University of Salford, United Kingdom.
- [2]. Aspen Technology V11.1, Cambridge, Massachusetts: Aspen Plus.
- [3]. Bugaje, I.M. (1987). *Solar-powered ammonia-water heat pump for refrigeration and air-conditioning applications*. (Unpublished M.Sc. Thesis). Ahmadu Bello University, Zaria, Nigeria.
- [4]. Cengel, Y.A. and Boles, M.A. (2007). *Thermodynamics: An Engineering Approach*, sixth ed. McGraw-Hill, New York.
- [5]. Demirel, Y. (2004). Thermodynamic analysis of separation systems. *Separation Science and Technology*, 39 (16), pp. 3897 – 3942.
- [6]. Demirel, Y. (2006). Retrofit of distillation columns using thermodynamic analysis. *Separation Science and Technology*, pp. 1 – 26.
- [7]. Dhole, V.R., and Linnhoff, B. (1993). Distillation column targets. *Computer and Chemical Engineering*, 17 (5-6), pp. 549 – 560.
- [8]. Holland, F.A., Pendyala V. R., Devotta S. and Watson, J.A. (1981a). Derived thermodynamic design data for heat pump systems operating on R-C318. Unpublished Technical Memorandum No. 43 of the Heat Pump Research Group of University of Salford, United Kingdom.
- [9]. Ognisty, T.P. (1995). Analyze distillation columns with thermodynamics. *Chemical Engineering Progress*, 91 (2), pp. 40 – 46.
- [10]. Olawale, A.S. and Adefila, S.S. (2011), Rankine heat pumps' performance equations as temperature-lift variables. *AIChE J.*, 57(7): 1905–1911. doi: 10.1002/aic.12396
- [11]. Olawale, A.S. and Adefila, S.S. (2012), Two-Parameter Rankine heat pumps' COP equations. *International Journal of Thermodynamics*, 15(2): 83–90. doi: 10.5541/ijot.360
- [12]. Pinto, F.S., Zemp, R., Jobson, M. and Smith, R. (2011). Thermodynamic Optimization of Distillation Columns. *Chemical Engineering Science* 66, 2920-2934. doi:10.1016/j.ces.2011.03.022
- [13]. Rashad, A. and El Maihy, A. (2009), Energy and Exergy Analysis of a Steam Power Plant in Egypt, Proceedings of 13<sup>th</sup> International Conference on Aerospace Science and Aviation Technology, ASAT – 13, May 26 – 28. <http://www.asat@mtc.edu.ng>
- [14]. SYSTAT (2002), *TableCurve 3D v4 for Windows User's Manual*, SYSTAT Software Inc., USA.
- [15]. U.S. Dept. of Energy, (1984) "Assessment of Potential Energy Savings in Fluid Separation Technologies: Technology Review and Recommended Research Areas", Office of Industrial Programs, Washington D.C., Document No. DOE/ID/1247634.
- [16]. Vuckovic, G.D., Vukic, M.V., Stojiljkovic, M.M., and Vuckovic, D.D. (2012). Avoidable and unavoidable exergy destruction and exergo-economic evaluation of the thermal processes in a real industrial plant. *Thermal Science*: 16 (2), pp. S433-S446.
- [17]. Yuehong B.I, Lingen, C. and Fengrui, S. (2010). Exergetic efficiency optimization for an irreversible heat pump working on reversed Brayton cycle. *Journal of Science*: 74 (3), pp. 351–363. Indian Academy of Science

Table 4: Coefficient values for the  $DX = f(H_2, H_5)$  Model for CAHP and  $[DX = f(h_A, H_A)]$  Model for Distillation Operation

Model Parameter	[DX = f(H <sub>2</sub> , H <sub>5</sub> )] Model for CAHP			[DX = f(h <sub>A</sub> , H <sub>A</sub> )] Model for Distillation		
	Value	Std Error	t-value	Value	Std Error	t-value
a	-0.77674	1.114368	-0.69703	0.588184	9.792381	0.060066
b	-80.2155	675.9666	-0.11867	-7.77366	14.85672	-0.52324
c	78.555	678.5875	0.115763	6.723359	18.782	0.357968
d	43.78763	131.9251	0.331913	-4.67993	84.39004	-0.05546
e	-42.4054	134.6821	-0.31486	4.011293	77.08471	0.052037
f	40.50992	114.467	0.353901	3.803114	35.87903	0.105998
g	-39.5067	120.5743	-0.32765	-4.398	29.57186	-0.14872
h	-30.1011	68.30905	-0.44066	2.467435	42.02385	0.058715
i	29.16088	71.90439	0.405551	-2.73107	48.71316	-0.05606
j	-12.1495	136.564	-0.08897	-0.98156	15.41612	-0.06367
k	11.64996	131.1154	0.088853	1.947654	16.70337	0.116602
l	16.97948	44.95445	0.377704	-0.64831	13.81344	-0.04693
m	-16.4992	41.31476	-0.39935	1.477748	25.65283	0.057606
n	5.717547	99.89768	0.057234	0.265233	7.25245	0.036572
o	-5.47391	97.41082	-0.05619	-0.8297	10.61667	-0.07815
p	-4.92046	60.62621	-0.08116	-0.15664	2.768366	-0.05658
q	4.746315	58.28212	0.081437	-0.28398	5.332944	-0.05325
r	-1.9869	14.4097	-0.13789	0.036105	1.79994	0.020059
s	1.887808	13.89249	0.135887	0.166828	3.259662	0.051179
t	1.996435	35.81818	0.055738	-0.07489	1.793275	-0.04176
u	-1.95081	35.04887	-0.05566	0.023153	0.66025	0.035067
v	1.114084	4.880477	0.228274	0.064858	0.796076	0.081473
aa	-1.08455	4.753724	-0.22815	-0.01192	0.556401	-0.02142